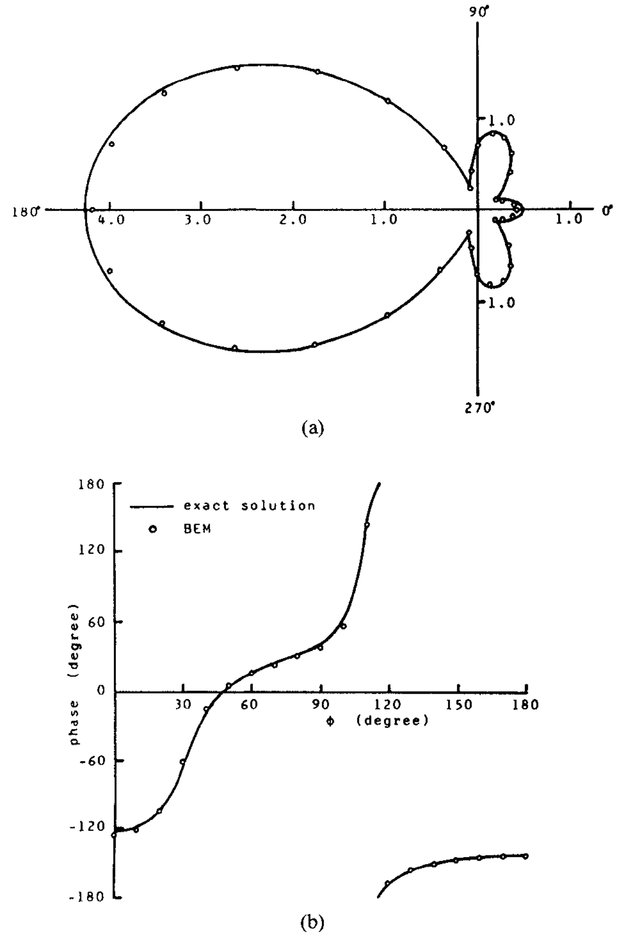

Fig. 13. E-wave scattering far-field pattern for dielectric circular cylinder in the case where E-wave incidents along x-axis in the negative x-direction. (a) Amplitude. (b) Phase.

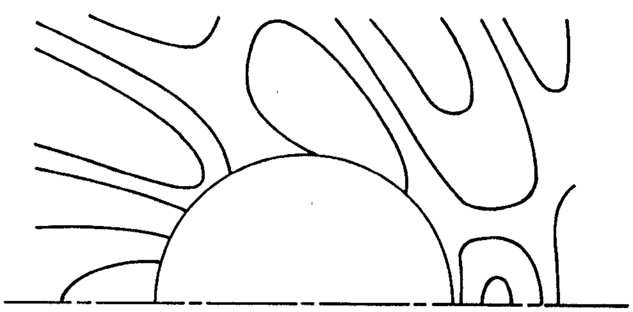

Fig. 14. The electric-field distribution around the dielectric circular cylinder.

FORTRAN program on a microcomputer, whose main CPU is MC68000 (8 MHz) and whose operating system is the UCSD p-system. Typically, the case of a parallel-plane waveguide having 40 nodes took about 20 m of CPU time.

VII. Conclusions

Application of the boundary-element method to electromagnetic-field problems was proposed. Several analyzing procedures for interesting cases were also given. The results obtained show that the boundary-element method is a very powerful numerical method for electromagnetic-field problems. Namely, by using the boundary-element method, far fewer nodes than by the finite-element method bring good accuracy, and unbounded field problems can be treated without any additional technique.

References

[1] B. H. McDonald and A. Wexler, "Finite-element solution of unbounded field problems," *IEEE Trans Microwave Theory Tech*, vol MTT-20, pp. 841–847, Dec. 1972.

[2] S. Washisu, I. Fukai, and M. Suzuki, "Extension of finite-element method to unbounded field problems," *Electron. Lett.*, vol. 15, pp 772–774, Nov. 1979.

[3] C A. Brebbia, *The Boundary Element Method for Engineers.* London: Pentech Press, 1978.

[4] C. A. Brebbia and S. Walker, *Boundary Element Techniques in Engineering.* London: Butterworth, 1980.

[5] S. Washisu and I. Fukai, "An analysis of electromagnetic unbounded field problems by boundary element method," *Trans. Inst. Electron. Commun. Eng. Jpn.*, vol. J64-B, pp. 1359–1365, Dec. 1981.

[6] S. Bilgen and A. Wexler, "Spline boundary element solution of dielectric scattering problems," in *12th Eur. Microwave Conf.*, (Helsinki, Finland), Sept. 1982, pp. 372–377.

[7] C. G. Williams and G. K. Cambrell, "Efficient numerical solution of unbounded field problems," *Electron. Lett.*, vol. 8, pp. 247–248, May 1972.

[8] S. W. Lee, "Ray theory of diffraction by open-ended waveguides. Part I," *J. Math. Phys.*, vol. 11, pp. 2830–2850, Sept. 1970.

[9] L. A. Vaynshteyn, *The Theory of Diffraction and the Factorization Method.* Boulder, CO: Golem, 1969.

[10] N. Okamoto and T. Kimura, "Radiation properties of H-plane two-dimensional horn antennas of arbitrary shape," *Trans. Inst. Electron. Commun. Eng. Jpn.*, vol. J59-B, pp. 25–32, Jan. 1976.

Optimum Design of a Potentially Dispersion-Free Helical Slow-Wave Circuit of a Broad-Band TWT

B. N. BASU, B. B. PAL, V. N. SINGH, AND N. C. VAIDYA

Abstract —**The results of an equivalent circuit analysis are studied for a potentially dispersion-free slow-wave circuit of a TWT which consists of a dielectric-supported helix in a metal shell provided with vanes. The optimum vane dimensions are predicted, which should be helpful in broadbanding the performance of a TWT.**

I. Introduction

With the advent of multi-octave-band traveling-wave tubes (TWT's), the study of dispersion shaping in the slow-wave structures of such tubes has become important [1]–[3]. In the case of a tube having a metal shell, dispersion can be reduced by placing the shell very close to the helix, but this will reduce the interaction impedance considerably. An alternative method would be to use a shell provided with metal vanes projected radially inward [1], [2]. In this case, the shell can be placed farther from the helix with the metal vanes allowed to approach the helix. The desired flat dispersion characteristics may be obtained by optimizing the radial dimension of the vanes.

In this paper, we present an optimum design curve relating the vane dimension and the location of the metal shell with respect to the helix, for different values of the helix wire radius. The curve is obtained by studying the dispersion relation of the circuit which can be derived using an equivalent circuit analysis.

Manuscript received April 26, 1983; revised October 31, 1983.

The authors are with the Centre of Research in Microwave Tubes, Department of Electronic Engineering, Institute of Technology, B.H.U., Varanasi-221 005, India

II. Equivalent Circuit Parameters and the Dispersion Relation

The analysis is carried out in the simple sheath-helix model. However, in order to add practical relevance to the problem, the effect of the finite thickness of the helix wire is taken into consideration. For real wire helices, the inner diameter of the dielectric support is considered to be a wire's diameter (thickness) larger than the mean helix diameter [4]. The system of supports for the helix considered here is a number of identical longitudinal dielectric wedge bars symmetrically arranged around the helix. Such a system of supports for the helix can be replaced by a dielectric tube of an effective relative permittivity interpreted in terms of the relative permittivity and dimensions of the support [5]. Thus, the mathematical model resolves down to that of a sheath helix surrounded by two tubes, one of relative permittivity unity corresponding to the free-space gap between the helix and the beginning of the dielectric, representing half the finite wire thickness of the helix [4], and the other of effective relative permittivity interpreted as above. Such a two-tube problem can be studied easily as a special case of a more general problem of a helix surrounded by any number of dielectric tubes [6].

As for the effect of a metal shell provided with radial vanes, it may be noted, since these vanes perturb only the longitudinal electric field, the inductance per unit length L of the line is unaffected by the presence of these vanes, but the capacitance per unit length C is modified as if the shell has no vanes but is brought closer to the helix at the position occupied by the tips of the vanes. This interpretation of line parameters is essentially based on the assumption that there are enough vanes so that the boundary formed by their tips is essentially an axially conducting cylindrical sheath which will effectively screen the longitudinal electric field but not the azimuthal electric field; the latter will be screened only by the overall metal shell [1].

Once the expressions for L and C have been obtained, these can be substituted in the transmission-line equation $\beta^2 = \omega^2 LC$, where β is the axial propagation constant, to obtain the following expression for the dispersion relation:

$$\left(\frac{k\cot\psi}{\gamma}\right)^2 = \left(\frac{I_0(\gamma a)K_0(\gamma a)}{I_1(\gamma a)K_1(\gamma a)}\right)D^2$$

where ψ is the pitch angle of the helix and D the dielectric loading factor of the structure given by

$$D = \left[\frac{1 + I_{0a}G/(K_{0a}H)}{1 - I_{1a}K_{1c}/(K_{1a}I_{1c})}\right]^{1/2}$$

where

$$G = \left[\left(1 + (\theta N)(\epsilon_r - 1)/(2\pi)\right)\left(1 + I_{1b_0}K_{0b}/(K_{1b_0}I_{0b})\right) - \left(1 - I_{0b_0}K_{0b}/(K_{0b_0}I_{0b})\right)\right]K_{0b_0}K_{1b_0}$$

$$H = -\left(1 + (\theta N)(\epsilon_r - 1)/(2\pi)\right)I_{0b_0}K_{1b_0} \cdot \left(1 + K_{0b}I_{1b_0}/(K_{1b_0}I_{0b})\right) - I_{1b_0}K_{0b_0}\left(1 - I_{0b_0}K_{0b}/(K_{0b_0}I_{0b})\right)$$

where

$I_{\nu r} = I_\nu(\gamma r)$ modified Bessel function of order $\nu(0,1)$ of the first kind,

$K_{\nu r} = K_\nu(\gamma r)$ modified Bessel function of order $\nu(0,1)$ of the second kind,

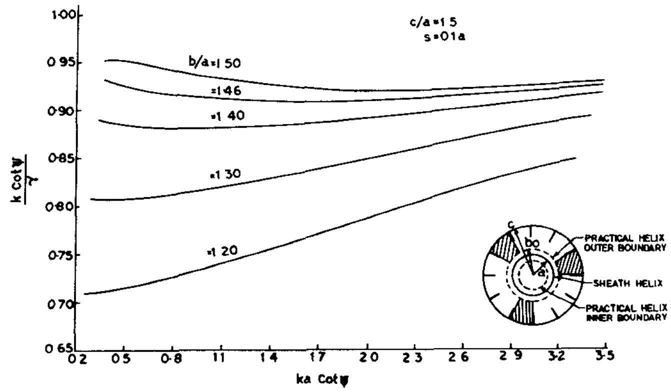

Fig. 1. Dispersion curves: $k\cot\psi/\gamma$, a quantity proportional to phase velocity versus γa, a quantity proportional to frequency, for different values of the vane dimension (b/a) and typical values of the shell-to-helix radius ratio (c/a) and the helix wire radius (s) ($\phi = 20°$ and $\epsilon_r = 6.65$ (Beryllia)).

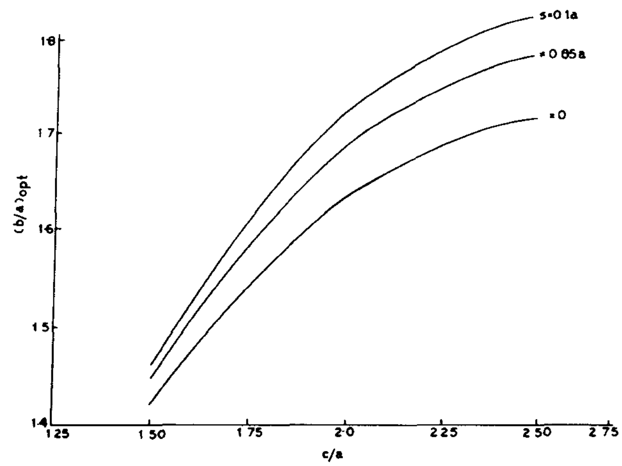

Fig. 2. Optimum vane dimension ((b/a) opt) versus shell to helix radius ratio (c/a) for different values of helix wire radius (s).

$\gamma = (\beta^2 - k^2)^{1/2}$ radial propagation constant,
k free-space propagation constant,
r radial coordinate,
a sheath helix radius = mean helix radius,
b_0 radius of the inner edge of the dielectric wedge bars,
b, c radial coordinates of the tips of the vanes and the metal shell, respectively, and
ϵ_r, θ, N relative permittivity of the dielectric-support material, wedge angle of the wedge-bar support, and number of supports, respectively.

III. Numerical Results and Discussion

Fig. 1 shows the effect of varying the radial dimension of the vanes (b/a) on the dispersion characteristics, for a typical location of the shell (c/a), and for a typical separation s $(= b_0 - a)$, between the mean position of the helix and the supports, representing half the thickness of the helix wire [4].

It may be seen from Fig. 1 that there exists an optimum vane-dimension $(b/a)_{opt}$ which would correspond to fairly dispersion-free characteristics. By studying similar plots for other various values of c/a and s (not shown here), we found that, in general, the flatness of these curves is reduced with the increase of the helix wire thickness. Fig. 2 shows the dependence of the optimum vane dimension on the location of the metal shell and the effect of the wire thickness thereupon.

Finally, it is of interest to make a comparison between the structures, with and without vanes, in respect of impedance of the circuit. For numerical appreciation, taking $s = 0$, $N = 3$, $C_r = 6.65$ (beryllia), $\theta = 20°$, $c/a = 2.5$, the optimum vane dimension corresponding to flat dispersion curves is obtained as $(b/a)_{\text{opt}} \approx 1.7$, for the structure with vanes (Fig. 2). For the vaneless structure, all other parameters remaining unchanged, flat dispersion characteristics result only when the shell is brought relatively close to the helix, to an optimum value; in this case, for $(c/a)_{\text{opt}} \approx 1.25$ [7]. Taking these optimized situations, and $\gamma a = 1.6$, the normalized characteristic impedances of the circuit, $2\pi(L/C)^{1/2}(\mu_0/\epsilon_0)^{-1/2}\tan\psi$, with and without vanes, come out to be 0.22 and 0.13, respectively.

References

[1] S. F. Paik, "Design formulas for helix dispersion shaping," *IEEE Trans. Electron Dev.*, vol. ED-16, pp. 1010–1014, 1969.

[2] J. L. Putz and M J. Cascane, "What's new in helix TWT's," in *IEDM Tech. Dig.*, 1979, pp. 526–529.

[3] J. P. Rymer and M. J. Cascone, "3 Octaves with one TWT," presented at Int. Electron Devices Meet. 1982, San Francisco, 13–15 Dec. 1982.

[4] D. T. Swift-Hook, "Dispersion curves for a helix in a glass tube," in *Proc Inst. Elec. Eng.*, vol. 105, 1958, pp. 747–755.

[5] L. N. Loshakov and E. B. Ol' derogge, "Propagation of slow electromagnetic waves along a helix with dielectric supports," *Radio Eng. Electron. Phys.*, vol. 13, pp. 45–51, 1968.

[6] B. N. Basu and A. K. Sinha, "Dispersion shaping using an inhomogeneous dielectric support for the helix in a travelling-wave tube," *Int. J. Electron.*, vol. 50, pp. 235–238, 1981.

[7] S. N Joshi and B. N. Basu, "Equivalent circuit analysis of a practical slow wave structure for TWT's," *J. Inst. Telecomm. Eng.*, vol 25, pp. 423–425, 1979.

Magnetostatic Forward Volume Wave Propagation—Finite Width

I. J. WEINBERG AND J. C. SETHARES, SENIOR MEMBER, IEEE

***Abstract*—The infinite radiation resistance [1] encountered at the low end of the magnetostatic forward volume wave frequency band for a YIG layer of finite width is avoided by employing a physically justifiable low frequency cutoff value higher than that for which radiation resistance would be infinite. Radiation reactance and insertion loss then can be calculated and are found to be relatively insensitive to the choice of the cutoff frequency, except for frequencies very close to cutoff. Beam spreading considerations determine the cutoff frequency.**

I. Theory

By considering Maxwell's equations with the magnetostatic approximation and the permeability tensor in the YIG region [2]

$$\bar{b} = \mu_0[\mu]\bar{h} \tag{1}$$

one obtains the potential function, in non-YIG regions, in the

Manuscript received July 11, 1983; revised November 21, 1983.

I. J. Weinberg is currently in the Air Force AFOSR University Resident Research Program, on leave from the University of Lowell, MA.

J. C. Sethares is with Rome Air Development Center, Hanscom AFB, MA 01731.

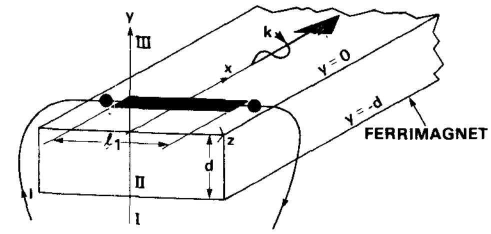

Fig. 1. Transducer geometry.

form

$$\psi = \int_{-\infty}^{\infty} e^{-ikx}\cos\frac{n\pi}{l_1}z\left(Ae^{\bar{k}y} + Be^{-\bar{k}y}\right)dk, \qquad n = 0,1,2,3\cdots \tag{2}$$

where k is the wave number in the x direction, l_1 is the strip width (Fig. 1), n represents the width mode and

$$\bar{k} = \sqrt{k^2 + (n\pi/l_1)^2}, \qquad n = 0,1,2,3,\cdots. \tag{3}$$

The components of $\bar{h}$ are found from the derivative of ψ. For $n = 0$, we have the infinite width case. For odd n, the potential vanishes at the strip ends $z = \pm l_1/2$.

For the YIG region, the potential function is taken from the basic equations to be in the form

$$\psi = \int_{-\infty}^{\infty} e^{-ikx}\cos\frac{n\pi}{l_1}z\left(A\cos\alpha\bar{k}y + B\sin\alpha\bar{k}y\right)dk, \qquad n = 0,1,2,3,\cdots \tag{4}$$

where, for forward volume waves [3]

$$\alpha = \left[-\left(1 + \frac{\gamma^2 HM}{\gamma^2 H^2 - f^2}\right)\right]^{1/2} \tag{5}$$

and

$$\gamma = 2.8\ \text{MHz/oe}, \quad M = 1750\ \text{oe}, \quad f = \omega/2\pi \tag{6}$$

and H is the biasing field magnitude.

Considering the case of no ground planes, we determine the constants in (2) and (4) for the three regions (Fig. 1) by requiring ψ to be finite at $y = \pm\infty$, b_y to be continuous at $y = 0$ and $y = -d$, h_x to be continuous at $y = -d$ and, for a given current distribution

$$h_{x\text{III}} - h_{x\text{II}} = J_z(x), \qquad \text{at } y = 0. \tag{7}$$

Application of boundary conditions yields the dispersion relation (see [3, eq. 17])

$$\left[(\alpha^2 - 1)\sin\alpha\bar{k}d - 2\alpha\cos\alpha\bar{k}d\right] = 0 \tag{8}$$

or

$$\bar{k} = \frac{1}{\alpha d}\tan^{-1}\frac{2\alpha}{\alpha^2 - 1} + \frac{m\pi}{\alpha d}, \qquad m = 0,1,2,3\cdots. \tag{9}$$

There are an infinite number of thickness solution modes, corresponding to the value of m, with $m = 0$ giving the fundamental mode.

By utilizing (8) and integrating (7) in the x direction, $-\infty$ to ∞, in the usual manner and integrating in the z direction, $-l_1/2$ to $l_1/2$, we obtain all constants in (2) and (4). Appropriate premultiple factors are used in these integrations.

0018-9480/84/0400-0463$01.00 ©1984 IEEE